Estuarine, Coastal and Shelf Science 85 (2009) 422–430

Contents lists available at ScienceDirect

Estuarine, Coastal and Shelf Science

journal homepage: www.elsevier.com/locate/ecss

Dynamics of heterotrophic dinoflagellates off the Pearl River Estuary, northern South China Sea

Wenlu Lan [a,b], Bangqin Huang [a,*], Minhan Dai [a], Xiuren Ning [c], Lingfeng Huang [a], Huasheng Hong [a]

[a] State Key Laboratory of Marine Environmental Science, Environmental Science Research Center, Xiamen University, Xiamen, PR China
[b] Marine Environmental Monitoring Center of Beihai, Bureau of Environmental Protection of Guangxi, Beihai, PR China
[c] Second Institute of Oceanography, State Oceanic Administration, Hangzhou, PR China

ARTICLE INFO

Article history:
Received 18 March 2009
Accepted 7 September 2009
Available online 16 September 2009

Keywords:
heterotrophic dinoflagellates
temporal and spatial variations
anticyclonic (warm) eddy
northern South China Sea

ABSTRACT

Variations in abundance, biomass, vertical profile and cell size of heterotrophic dinoflagellates (HDFs) between summer and winter and its controlling factors were studied in the northern South China Sea (SCS). It was found that HDF abundance and carbon biomass were 4–102 $\times 10^3$ cells L^{-1} and 0.34–12.3 mg C L^{-1} in winter (February 2004), respectively, while they were 2–142 $\times 10^3$ cells L^{-1} and 0.22–31.4 μg C L^{-1} in summer (July, 2004), respectively, in the northern SCS. HDF abundance and carbon biomass decreased from the estuary to inshore and then offshore. Vertical profiles of HDF abundance were heterogeneous, which accorded well with that of chlorophyll a (Chl.*a*). Higher abundance of HDFs was often observed at a depth of 30–70 m offshore waters, matching well with the Chl.*a* maximum, while it showed high abundance at the surface in some coastal and estuary stations. Small HDFs (≤20 μm) dominated the assemblage in term of abundance accounting for more than 90%. However, large HDFs (>20 μm) generally contributed equally in terms of carbon biomass, accounting for 47% on average. HDFs showed different variation patterns for the different study regions; in the estuarine and continental shelf regions, abundance and biomass values were higher in summer than those in winter, while it was the reverse pattern for the slope waters. Hydrological factors (e.g. water mass, river outflow, monsoon and eddies) associated with biological factors, especially the size-fractionated Chl.*a*, seemed to play an important role in regulating HDF distribution and variations in the northern South China Sea.

1. Introduction

Heterotrophic dinoflagellates (HDFs) are a major component of the micro-zooplankton (<200 μm) size class, and as predators of various classes of plankton, and as prey for larger members of the zooplankton, they provide a key trophic linkage in the microbial food web (e.g. Jeong, 1999; Levinsen and Nielsen, 2002; Yang et al., 2004; Sherr and Sherr, 2007). Sherr and Sherr (2007) have summarized evidence showing that HDFs are a significant component of micro-zooplankton and they have the greatest potential to consume diatoms of the major groups of herbivores in pelagic systems. Since many species have an optimal size ratio between themselves and their prey of 1:1, HDFs can prey on organisms as large as, or larger than, themselves in size, while other categories of phagotrophic protists (heterotrophic flagellates and ciliates) in general feed on smaller sized prey (e.g. Jeong 1999; Sherr and Sherr, 2007). Consequently, small HDFs (<20 μm) can compete for prey with heterotrophic nanoflagellates and ciliates, and large HDFs (>20 μm) can compete with copepods for prey (Archer et al., 1996; Sherr and Sherr, 2007). A certain part of the phytoplankton standing stock is consumed by HDFs and so primary production is affected (Hall et al., 2004; Hlaili et al., 2006). Moreover, with their potential fast-growth rate, HDFs respond quickly to blooms and play a role as significant as the meso-zooplankton in consuming phytoplankton blooms (Archer et al., 1996; Assmy et al., 2007; Sherr and Sherr, 2007). Thus, it is certain that HDFs play a significant role in carbon-energy flow and material cycling in oceanic ecosystems (Lessard, 1991; Sherr and Sherr, 1994; Jeong 1999).

Although the important role of HDFs in pelagic microbial food web dynamics is documented in numerous equatorial to polar studies (e.g. Verity et al., 1996; Sherr et al., 1997; Levinsen and Nielsen, 2002; Yang et al., 2004; Henjes et al., 2007), many reports are still biased towards the ciliated component of the micro-

* Corresponding author. Environmental Science Research Center, Xiamen University, Xiamen, Fujian 361005, PR China.
E-mail address: bqhuang@xmu.edu.cn (B. Huang).

0272-7714/$ – see front matter © 2009 Elsevier Ltd. All rights reserved.
doi:10.1016/j.ecss.2009.09.008

zooplankton rather than HDFs (Nielsen and Andersen, 2002; Sherr and Sherr, 2007). In addition, misconceptions remain that the micro-zooplankton planktonic protists are mainly ciliates (Sherr and Sherr, 2007). Based on the important roles described above, the HDFs obviously deserve to be included in studies of micro-zooplankton community structure and food web dynamics (Sherr et al., 1997; Nielsen and Andersen, 2002; Sherr and Sherr, 2007). However, spatial distribution and temporal variations of these assemblages are not adequately addressed.

The northern South China Sea (SCS) off the Pearl River estuary, located mainly between 17 and 23 °N and from 110 to 118 °E, and characterized by tropical and subtropical climate is a marginal sea with wide continental shelves and complex hydrological environments. The northern SCS represents typical oligotrophic characteristics, with significant environmental gradients (e.g. temperature, salinity and nutrients) due to the influence of the Pearl River, the thirteenth largest river in the world. The northern SCS is also sensitive to many types of physical forcing on the different terms (e.g. meso-scale eddies, monsoon). Previous studies show that the oligotrophic offshore regions of the northern SCS are characterized by low biomass and special temporal variations with high biomass in winter while low in summer, which are quite different from the conditions in temperate and tropical waters (Tseng et al., 2005; Huang et al., 2008). Thus it is necessary to assess micro-zooplankton stocks in order to study the coupling of predator–prey in such a subtropical oligotrophic ocean. However, there has been little study concerning micro-zooplankton distribution and temporal variation in this area. Eddies are very active in the northern SCS (e.g. Wang et al., 2003; Jia et al., 2005). Ning et al. (2004) report that eddies affect phytoplankton and primary production in the SCS, indicating that the cold eddy shows rich nutrients, low dissolved oxygen (DO), and high Chl.*a* and primary productivity (PP), while the warm pool is associated with poor nutrients, high DO, and low Chl.*a* and PP. Unfortunately, very few studies have been made concerning the effects of eddies on HDF abundance and biomass in this area. Two anticyclonic (warm) eddies occurred during our cruise in February, 2004, and two transects were set across the two warm eddies to study coupling between meso-scale eddies and HDFs.

The aim of the present study was to examine temporal and spatial variations of HDFs and the factors influencing their distribution and temporal variations. The coupling between meso-scale eddies and HDFs, and the size-spectrum of HDFs were also addressed in the northern SCS.

2. Materials and methods

2.1. Study area

The study was carried out during two cruises, which were in February 2004 and July 2004, in the northern SCS off the Pearl River Estuary (17.5–23 °N, 110.5–118 °E). The study area involved subtropical waters with wide continental shelves and very complex hydrological conditions. Stratification existed almost throughout the year offshore, although the study area was influenced by the East Asian monsoon. Differences of wind velocity and other hydrological factors (e.g. meso-scale eddies and upwelling) cause changes in the vertical mixing layer nutricline depth (Tseng et al., 2005), influencing nutrient supply and availability in the upper water, and affecting plankton biomass and distribution in the study area concomitantly. The outflows of the Pearl River and the Hanjiang River also greatly influence this area, mostly in the wet season (March–September), and provide large amounts of nutrients into this area (Huang et al., 2008). Based on the water depth along the transects, we divided the area into three typical regions: coast, shelf, and slope.

The sampling stations are shown in Fig. 1. There were four transects (A, B, C and D), which went southeastward from the coast to the continental shelf and then to the slope (deep water). Transect A was from the Pearl River estuary to the southwest of Dongsha Island; transect B passed through the summer wind-driven upwelling off eastern Guangdong; transect C was from Modaomen, one branch of the Pearl River to the SCS, to the continental slope; while transect D was to the northeast of Hainan Island.

During the winter cruise in February, 2004, two anticyclonic (warm) eddies were observed (Fig. 1). Transect B partly cut through one warm eddy (WE1) near Dongsha Island, while transect D cut through another warm eddy (WE2) to the east of Hainan Island. WE1 was stronger and was formed by the Kuroshio intrusion while WE2 was in its weakening period and might have been of local origin from the northern SCS (Wang et al., 2008). Stn. B2 was at the edge of WE1, while Stn. D3 was at the edge of WE2.

2.2. Sampling

Water samples for biological and chemical analyses were collected using Niskin bottles from the Sea Bird 19 CTD-sampler (Oceanic Co., USA), at 3–8 selected depths for each station depending on the water depth. Biological and chemical analyses were carried out on water samples drawn from the same bottles.

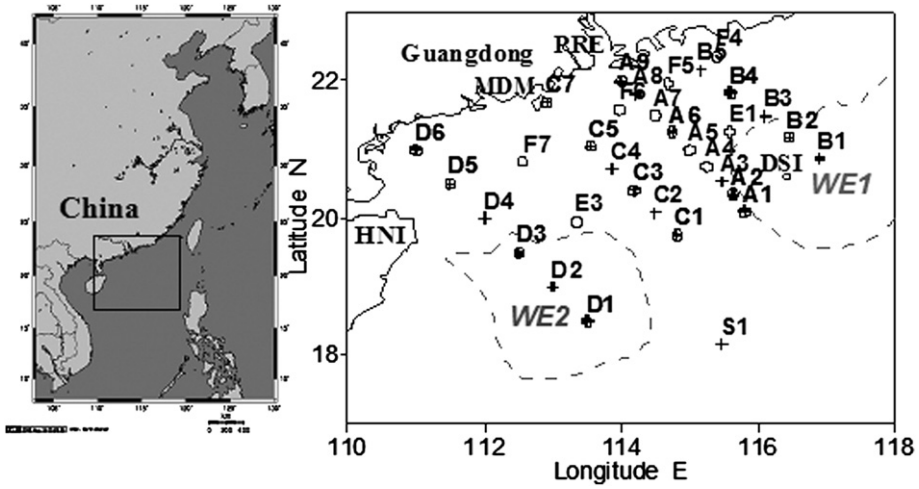

Fig. 1. Sampling stations in the northern South China Sea. + for July, 2004, and ○ for February, 2004. PRE, Pearl River Estuary; MDM, Modaomen; HNI, Hainan Island; DSI, Dongsha Island; WE1, warm eddy 1; WE2, warm eddy 2.

2.3. Hydrological data

At each station, the Sea-Bird 19 CTD profiler was used to obtain vertical profiles of temperature, salinity, density and fluorescence. Just prior to the cruise, the CTD was shipped back to Sea-Bird for calibration. Data from the sensors of the CTD units were obtained during downcast. Data processing followed the JGOFS protocol (Knap et al., 1996).

2.4. Nutrient analysis

Water samples were filtered using 0.45 μm Nuclepore filters. The filtrate was frozen and nutrients were measured within 24 h. Nitrite and phosphate were determined colorometrically using a flow injection analyzer (Tri-223 auto analyzer) (Pai et al., 1991). Nitrate plus nitrite was measured by reducing nitrate to nitrite with an on-line Cd coil (Pai et al., 1991). All these measurements were undertaken onboard immediately upon sample collection. The precision was 0.61% for phosphate (at 1.2 μM) and 0.57% for nitrite (at 2.4 μM). The detection limit was 0.1 μM for phosphate and 0.5 μM for nitrate.

2.5. Chlorophyll a

Chlorophyll *a* (Chl.*a*) was determined using fluorescence analysis (Parsons et al., 1984), with the volume of seawater sample being 300–1000 mL, depending on the Chl.*a* concentration, and *in vitro* measurements were conducted using a Shimadzu (RF-5301PC) fluorospectrometer with the excitation and emission wavelengths set at 430 and 670 nm, respectively. The Chl.*a* content of the different size classes (pico-, nano- and micro-) of the phytoplankton were measured based on the size-fractionation of water samples as described in Huang et al. (1999).

2.6. Enumeration of HDFs

In the case of the small HDFs with size ≤20 μm, a 100 mL sample was size-fractionated through a 20 μm nylon mesh, and then preserved with 0.5% glutaraldehyde (Yang et al., 2004). The samples were stored cold (<4 °C) until filtration. The samples were stained with DAPI (4′6′-diamidino-2-phenyl-indole, 25 μg mL^{-1} final concentration) and filtered by gravity onto a black-stained polycarbonate membrane filter with 2 μm pore size. A backing filter of 5 μm pore size was used to promote the even distribution of material on the filter. The filter was transferred to a microscope slide and embedded between two drops of paraffin oil. A cover slip was placed on top of the second drop of oil, and the prepared slides were immediately stored in darkness at −20 °C onboard until they were returned to the laboratory for later analysis. Filters were examined using an epifluorescence Leica compound light microscope with ×400 and/or ×1000 magnification. At least two hundred HDF cells were examined.

For HDFs >20 μm, a 500–1000 mL water sample was fixed with glutaraldehyde (1% in final concentration) and held in darkness at 4 °C. The fixed sample was condensed to 10 mL by settling and the upper water was siphoned off through a 10 μm mesh. Then a 1 mL subsample was placed in a counting chamber for enumeration under the inverted fluorescence microscope (LEICA DMIL, ×200). A 10 μg mL^{-1} final concentration of DAPI was added to the chamber for 7 min, and the whole slide was enumerated. Several subsamples were examined and at least one hundred >20 μm HDF cells were counted (with the exception of a few samples with very low abundance).

Dinoflagellates were distinguished from other flagellates based on cell morphology and nucleus structure, especially the unique condensed chromosomes visible with DAPI staining (Verity et al., 1996). HDFs were distinguished from autotrophic taxa by the absence of chlorophyll fluorescence in the fixed samples which were analyzed. Each HDF cell counted was sized for bio-volume calculation using a calibrated ocular micrometer. The calculation of carbon biomass of HDFs was based on the equation: carbon (pg) = 0.216×[volume, μm^3]$^{0.939}$ (Menden-Deuer and Lessard, 2000). Depth-integrated carbon biomass was calculated from the surface to the bottom layer in coastal and continental shelf water based on depth, and from the surface to 200 m over the continental slope.

2.7. Data analysis

The statistical differences between HDF biomass and environmental parameters were evaluated using one-way ANOVA. The Bonferroni test was selected for multiple comparisons of ANOVA when equal variances were assumed; otherwise the Games-Howell test was employed. p Values <0.05 were regarded as the significant level. Correlations between HDFs and environmental variables were determined by bivariate correlation using the Pearson correlation coefficient. Correlation analysis was performed for all sample depths from each station. All tests were performed using SPSS 13.0 software.

3. Results

3.1. Environmental parameters in the study area

The temporal and spatial distribution of temperature, salinity and Chl.*a* in the surface water and in a typical transect (Transect A) of the study area during the winter and summer cruises have been described in Huang et al. (2008). The stations were divided into the three sub-regions: estuary and coast (Stns A9 and C7); continental shelf waters; and slope waters at depths of ≤50 m, >50–≤100 m and >100 m based on the topography of the study area (Huang et al., 2008). The estuarine and coastal water system was characterized by lower salinity, lower temperature and higher Chl.*a*, while relatively higher temperature, higher salinity and lower Chl.*a* identified the slope water.

Sea surface temperature (SST) increased from the estuary to the continental shelf to the slope water, with higher value in the summer (27.44–31.02 °C) than in the winter (15.56–24.53 °C). Salinity of the surface water showed a similar trend to SST, with values which varied between 31.24 and 34.92 in the winter and between 20.18 and 34.52 in the summer. Chl.*a* in the surface water decreased from estuary to continental shelf and then to the slope water in both seasons, which showed a contrary trend to SST and salinity. In the surface water in summer, high temperature (>30 °C), relatively low salinity (<33) and high Chl.*a* were observed in continental shelf water in the middle of transect B at Stns B3 and B4. The highest Chl.*a* value was observed in the surface layer of the slope waters (at Stn. D3), with a value greater than 1.0 μg L^{-1} (Huang et al., 2008).

Vertical profiles of temperature were homogeneous in coastal water but heterogeneous in the shelf and slope waters, and the thermocline was weak in continental shelf and slope waters in winter. In the summer, an apparent thermocline occurred between about 10–50 m and 40–70 m in the continental shelf and slope waters respectively. Salinity in the upper water of transect A was more homogeneous during the winter. Chl.*a* was higher in the winter in the upper water offshore while in coastal water it was higher in the summer. It was higher in the bottom water than at the surface at the inner shelf stations, while sub-surface Chl.*a* maximum (SCM) layer occurred at about 40–70 m in most of the off

shelf stations and was mainly contributed by the pico-phytoplankton (Huang et al., 2008).

3.2. Horizontal distribution and temporal variations of HDFs

Abundance and carbon biomass of HDFs and their horizontal distribution are shown in Fig. 2 and Table 1. HDFs were ubiquitous in the northern SCS and their abundance and carbon biomass ranged from 4×10^3 to 102×10^3 cells L^{-1} and from 0.34 to 12.3 μg C L^{-1} in winter; and from 2×10^3 to 142×10^3 cells L^{-1} and from 0.22 to 31.4 μg C L^{-1} in summer. High abundance of HDFs was observed in estuarine and coastal waters with a value of approximately 100×10^3 cells L^{-1}, with the highest values in the estuary area, at the bottom of Stn. C7 in winter and at the surface of Stn. A9 in summer. The abundance in surface water ranged from 11×10^3 to 94×10^3 cells L^{-1} with a mean of $32\pm19\times10^3$ cells L^{-1} ($n=21$) in winter, while in summer it ranged from 8×10^3 to 142×10^3 cells L^{-1} with an average of $37\pm30\times10^3$ cells L^{-1} ($n=24$). Abundance decreased from the coast to the slope waters (Fig. 2a, b). However, a relatively high abundance of HDFs was observed on the continental shelf around Stn. B4 and on the slope around Stn. D3 in summer (Fig. 2b). The abundance was low (less than 20×10^3 cells L^{-1}) at most stations in the slope waters in both seasons (Fig. 2a, b). Highest abundance of HDFs in the surface of the slope water was located at Stn. B2 in the winter but at Stn. D3 in the summer, with values of 44×10^3 and 54×10^3 cells L^{-1}, respectively.

The depth-integrated (≤200 m) carbon biomass of HDFs ranged from 134 to 458 mg C m^{-2} in the winter and from 163 to 657 mg C m^{-2} in summer (Fig. 2c, d). High depth-integrated HDF biomass was observed on the slope in the winter but on the shelf in the summer. Integrated HDF carbon biomass generally increased from coastal to offshore water in the winter, while it generally decreased from continental shelf stations to the coastal and the slope water in the summer (Fig. 2c, d).

Variations of HDF biomass between summer and winter varied at different regions in the northern SCS (Table 1). For estuarine and coastal water, HDF abundance was similar between the two seasons, while carbon biomass was higher in the summer ($p<0.05$). For the continental shelf, HDF abundance and carbon biomass (including integrated) were higher in the summer ($p<0.05$). However, for the slope water, HDF abundance and biomass were significantly higher in winter ($p<0.01$, Table 1).

3.3. Vertical distribution of HDF abundance and carbon biomass

Fig. 3a, b shows the distribution of HDF abundance along transect A in winter and summer. High abundance occurred in coastal waters, and generally decreased from coastal to slope waters. HDF abundance also decreased from surface to deeper water in the slope water and high abundance was mostly concentrated in the upper 100 m. HDFs were rare below 100 m, with abundance values less than 10×10^3 cells L^{-1} (excluding Stn. D1 in winter). However, in continental shelf and some coastal waters, HDFs generally increased from surface to bottom and maximum HDF abundance in the water profile was mainly concentrated in or up to the SCM layer (about 40–70 m). The HDF distribution pattern along each transect

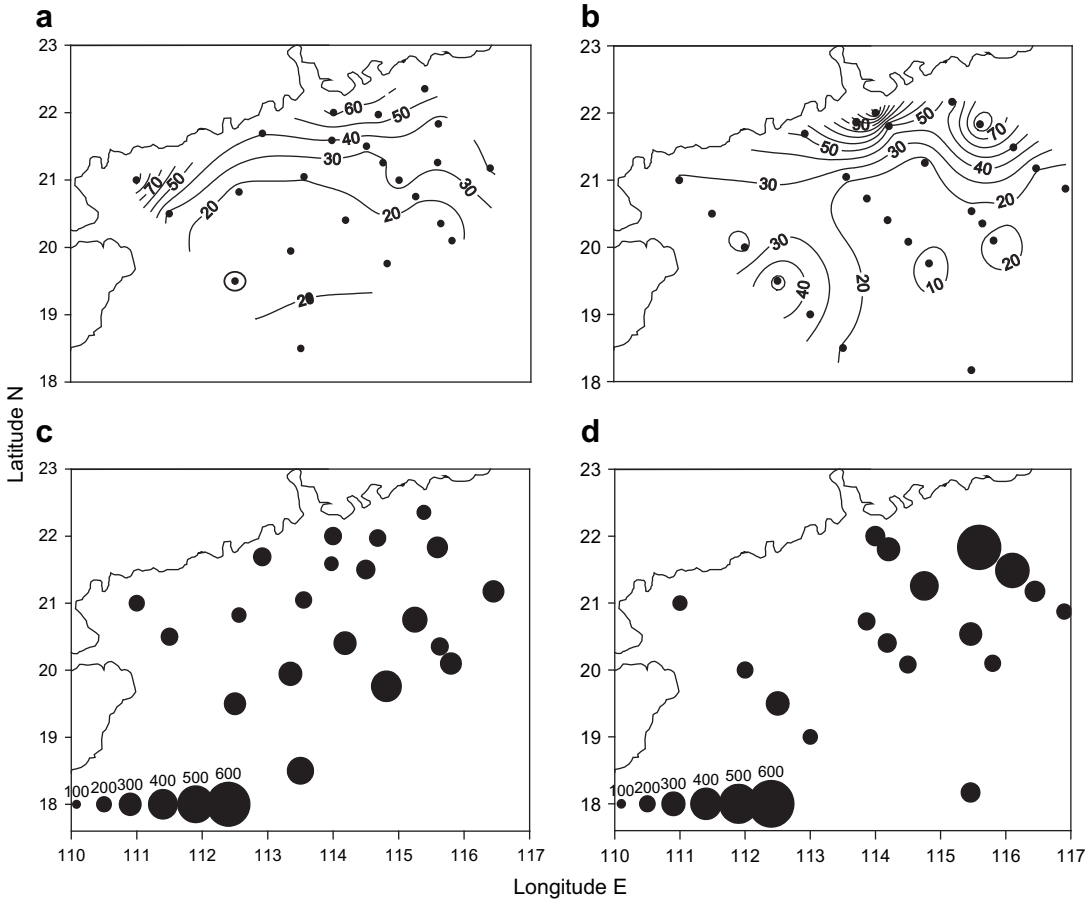

Fig. 2. Horizontal distribution of heterotrophic dinoflagellates in the northern South China Sea. Abundance ($\times10^3$ cells L^{-1}) in surface water in (a) winter, (b) summer; and water-column integrated biomass (≤200 m, mg C m^{-2}) in (c) winter, and (d) summer.

Table 1
Average (±SD) abundance and carbon biomass of the heterotrophic dinoflagellates in the northern South China Sea during cruises in February and July 2004. Note: integrated biomass was calculated water column integrated within 200 m.

Regions	Abundance (10^3 cells L^{-1})	Carbon biomass ($\mu g\,C\,L^{-1}$)	Integrated biomass ($mg\,C\,m^{-2}$)
Feb. 2004			
Estuary and coast	51.7 ± 27.3	8.4 ± 3.4	184 ± 52
Continental shelf	28.1 ± 11.0	3.8 ± 1.2	265 ± 37
Continental slope	19.6 ± 10.1	2.7 ± 1.4	312 ± 70
Jul. 2004			
Estuary and coast	53.0 ± 32.1	11.5 ± 9.7	229 ± 64
Continental shelf	32.7 ± 25.0	4.7 ± 1.8	391 ± 189
Continental slope	13.4 ± 11.2	1.9 ± 1.2	266 ± 54

was similar in both seasons (figures not shown). However, in transect B in the summer (figure not shown), high abundance of HDFs was concentrated at the shelf stations, and maximum abundance was observed at the water surface and decreased from surface to bottom.

Distribution trends of HDF carbon biomass in both seasons were similar to abundance, with high biomass in estuarine and coastal water and decreased levels in continental shelf and slope water. No direct trend of vertical variation was observed for HDF carbon biomass in the Pearl River estuary and coastal water in either season. In continental shelf water, HDF biomass increased from surface to sub-bottom in the winter and to the bottom of the water column in the summer. In the slope region as well as at Stn. S1 in the oceanic basin, a sub-surface HDF maximum was ubiquitous at a depth of about 30–70 m and biomass was very low below 100 m in both seasons.

3.4. Size-fractionated HDFs from estuary to shelf and slope

The HDF assemblage was classified as containing both small (≤20 μm) and large HDFs (>20 μm) in the present study. At all depths sampled in both February and July, the majority of HDFs were of small size. The abundance of small HDFs accounted for 91.8–99.2% (average 96.3%) of the total HDFs in the winter, while it contributed 90.0–99.4% (average 95.8%) in the summer. The contribution of small HDFs generally increased from coastal to slope waters, both in terms of abundance and biomass, while large HDFs showed the opposite trend (Fig. 4). Despite their overwhelming numerical dominance, the small HDFs, however, did not dominate the HDF biomass in all samples (mean = 53%; range = 32–80%). The large HDFs represented 20–62% of the HDF biomass in winter and 30–65% in summer (Fig. 4). The contribution of small HDFs to the total HDF biomass was high at the slope stations with the highest value at Stn. B2 in winter, and low at coastal stations with the lowest value at Stn. A9 in the estuary in summer.

The HDF assemblage was numerically dominated by athecate dinoflagellates in the winter. Thecate HDFs were present at concentrations less than 0.2×10^3 cells L^{-1}, contributing very little to the HDF abundance in both seasons. In both February and July 2004 in the northern SCS, the dominant morphotypes in terms of abundance were *Gymnodinium*/*Gyrodinium*-shaped cells of 8–15 μm diameter, that is small HDFs. Morphotypes of spindle- or fusiform-shaped cells less than 20 μm in length were the second most abundant type of small HDFs. Large size *Gyrodinium* spp., and thecate *Protoperidinium* spp. and *Diplopsalis* types were predominant in the *Gyrodinium* large HDFs.

3.5. Comparison of vertical profiles of HDFs between the different warm eddies

Vertical distributions of HDFs were heterogeneous among the two warm eddies with different origins (at Stns B2 and D3) as well as the reference station (at Stn. C3, without the influence of the warm eddy in the shelf waters of the northern SCS) (Fig. 5).

At the reference station (Stn. C3), HDF abundance was low in the surface layer, increased in the sub-surface layer at a depth of ~50 m, and then decreased with depth (Fig. 5a). At WE2 (Stn. D3) vertical distribution was similar to the reference station, and abundance was very low ($<10 \times 10^3$ cells L^{-1}) in the surface water, reached a maximum at 50 m and then decreased below this (Fig. 5b). However, HDFs were concentrated in the surface layer in WE1 (Stn. B2), with an abundance of 44×10^3 cells L^{-1} (Fig. 5c), which was approximately 4–5 fold that at the reference station and at Stn. D3 in WE2. Thereafter, HDF abundance in WE1 decreased with depth (though a relatively high value occurred at 70 m) which was different to the pattern at both the reference station and the WE2 station.

3.6. Correlation between HDF biomass and other parameters

Tables 2 and 3 show correlation values between HDF biomass and physical–chemical and biological parameters in the mixing

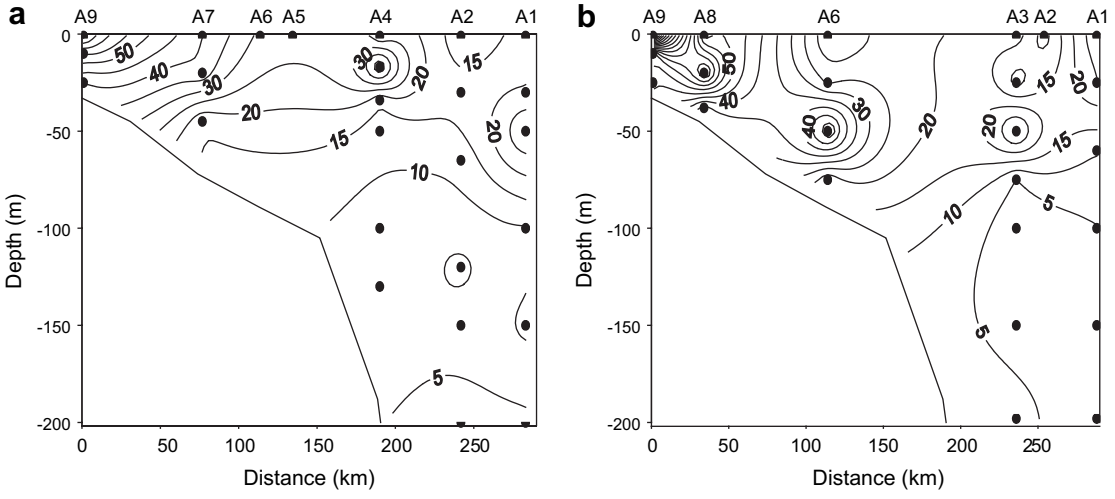

Fig. 3. Distribution in abundance of heterotrophic dinoflagellates ($\times 10^3$ cells L^{-1}) along transect A in February 2004 (a) and July 2004 (b).

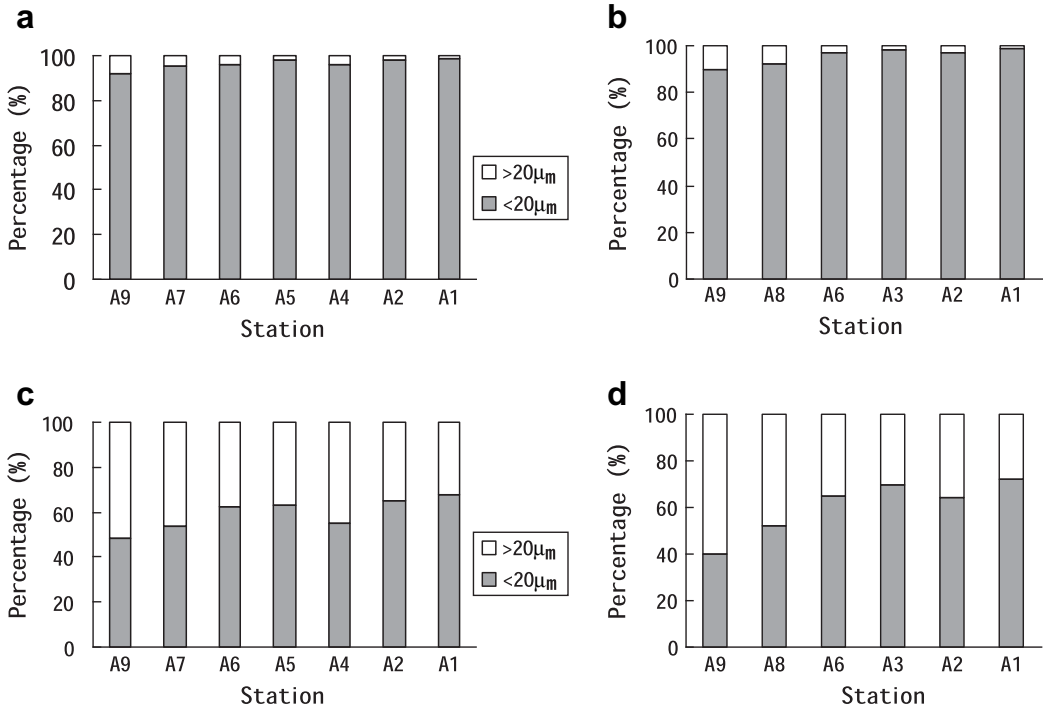

Fig. 4. Size structure of abundance (upper panels) and carbon biomass (lower panels) of heterotrophic dinoflagellates along transect A in the winter (left panels) and summer (right panels).

layer and at all sampling depths (in the upper waters of less than 200 m depth) in both seasons.

Negative correlations were observed between HDF biomass and temperature, and HDFs and salinity, in the mixing layer in the both seasons except for HDF and temperature in the summer (Table 2). HDF biomass was significantly positively correlated with nitrate in the mixing layer in both seasons, but correlated more significantly with Chl.*a* in the mixing layer both in winter and summer. For the overall samples, HDF biomass was negatively correlated with salinity and nitrate and positively correlated with Chl.*a* in both seasons. As in the mixing layer, correlations between HDF biomass and Chl.*a* were the most significant (Table 2).

The results also showed significant positive correlation between HDF biomass and size-fractionated Chl.*a* biomass in both seasons (Table 3). Small HDF biomass was significantly correlated with the nano- and pico-phytoplankton, whereas large HDF biomass was significantly correlated with micro-, nano-, and pico-phytoplankton biomass. Total HDFs significantly correlated with micro-, nano- and pico-phytoplankton biomasses and was correlated most significantly with nano- and pico-phytoplankton biomass.

4. Discussion

4.1. Comparison with other sea areas

The present study was the first to address temporal and spatial distribution, vertical profiles, and size structure of HDFs in the northern SCS. The abundance and biomass in the present study were comparable to those previously reported from other similar regions of the world (see Table 4) and in the range for coasts and oceans reported by Jeong (1999). Small HDFs made a primary contribution to both HDF abundance and biomass on the continental shelf and slope in the northern SCS, which was again comparable to similar regions (Table 4). Our results also showed that distance from the coast to the open ocean characterized the distribution gradients of HDFs in this study area. These trends were

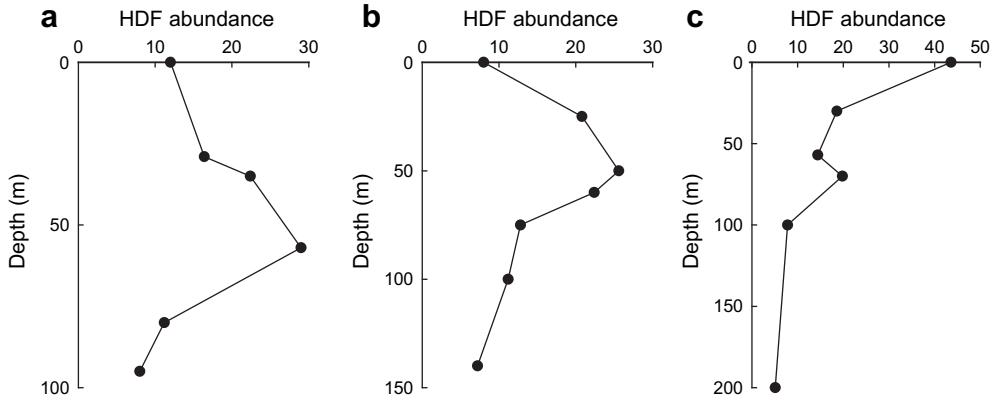

Fig. 5. Vertical profiles of abundance (10^3 cells L^{-1}) of heterotrophic dinoflagellates in the reference station (a, at Stn. C3), warm eddy 2 (b, at Stn. D3), and warm eddy 1 (c, at Stn. B2).

Table 2
Pearson correlation coefficients between the heterotrophic dinoflagellate (HDF) and environmental parameters in the northern South China Sea during cruises in February and July 2004.

HDF	Temperature	Salinity	Nitrate	Phosphate	Chl.*a*	*n*
Feb. 2004						
Mixing[c]	−0.509[b]	−0.468[b]	0.472[b]	–	0.671[b]	45
All[d]	−0.271[a]	−0.521[b]	−0.256[a]	−0.235	0.653[b]	69
Jul. 2004						
Mixing[c]	0.131	−0.382[a]	0.561[b]	–	0.715[b]	35
All[d]	0.359[b]	−0.388[b]	−0.409[b]	−0.019	0.613[b]	61

Significant correlation was defined as: [a]$p < 0.05$; [b]$p < 0.01$.
[c] Samples in mixing layer.
[d] Samples in layers of <200 m depth; – not enough data for regression analysis.

similar to those found in phytoplankton and nanoflagellates in the same cruise in the northern SCS (Huang et al., 2008) and agreed with trends of HDFs as well as with other nano- and micro-zooplankton in other studies (Stelfox et al., 1999; Rat'kova and Wassmann, 2002; Chou et al., 2005).

Vertical profiles varied and depended on the different waters in the northern SCS during the winter and summer in the present study. This agreed well with the variable vertical distribution of HDFs seen in other regions of the world. High abundance and biomass of HDFs in coastal and continental regions were generally below the pycnocline and near the bottom, which was similar to the results of Nielsen and Andersen (2002) in estuarine, and Stelfox et al. (1999) in nearshore regions. In deep water, HDF abundance and biomass were concentrated in the mixed surface layer and generally higher in the SCM layer, and this accorded well with the results of other work on deep water (Lessard and Murrell, 1996; Sherr et al., 1997; Yang et al., 2004). Overall, despite variable distribution in different water profiles, vertical distribution of HDFs was mostly in accordance with the vertical distribution of Chl.*a*, and thus agreed well with previous studies in other waters (e.g. Lessard and Murrell, 1996; Sherr et al., 1997; Nielsen and Andersen, 2002; Yang et al., 2004). Significant correlation between micro-zooplankton groups and phytoplankton biomass suggested a strong trophic link between these predators and their prey (Yang et al., 2004). During this study, HDF biomass appeared to show significant correlation with Chl.*a* concentration ($p < 0.01$), and this suggested that HDFs may play a pivotal role in organic matter cycling in the northern SCS.

4.2. The effects of warm eddies on HDFs

During the past ten years, oceanographers have studied the coupling between physical and biological processes (Lewis, 2002). However, the effect of warm eddies on the micro-zooplankton is poorly known. The micro-zooplankton assemblage in a warm eddy was examined only during dilution experiments on the surface water in the Atlantic sector of the Southern Ocean by Froneman and Perissinotto (1996), and in the surface and DCM layer in the eastern Indian Ocean by Paterson et al. (2007). The present study was the first one concerning the effects of warm eddies on the structure and vertical distribution of HDF assemblages.

Our results showed that the vertical profile of the HDFs was quite different in the two warm eddies (Fig. 5), indicating that the effects of warm eddies on HDF distribution in the water column differed among eddies. Meso-scale eddies play an important role in horizontal and vertical mixing of water as a hydrological event, and thus influence nutrient availability and variability of biological parameters (Falkowski et al., 1991; Mackas and Galbraith, 2002; Benitez-Nelson et al., 2007; McGillicuddy et al., 2007). However, the effects of warm eddies on biological parameters are complicated, and they display different effects on the plankton (e.g. Rodríguez et al., 2003; de Souza et al., 2006; Paterson et al., 2007). During our study, the two warm eddies had different origins and ages, and this affected the plankton biomass and community structure differently. Huang et al. (in press) show that in the WE1, which is shed by the Kuroshio intrusion and is characterized by oligotrophic conditions, prochlorophytes dominate the phytoplankton community, while in the WE2, which is shed from the coastal waters of the northern SCS, haptophytes dominate the euphotic zone. Due to their down welling nature, warm eddies are expected to isolate nutrient depleted water at the surface (McGillicuddy and Robinson, 1997), which presumably supports the microbial food web through nutrient regeneration (Paterson et al., 2007). In the present study, small HDFs dominated both in WE1 and WE2, with a higher contribution in WE1, which might be due to the Kuroshio origin of WE1. HDF abundance in WE2 was no different to that of the reference station because of local origin and age. High abundance of small HDFs at the surface of Stn. B2 and at the DCM layer at Stn. D3 should be due to the large available food resource of pico- and nano- phytoplankton as well as nanoflagellates (Huang et al., 2008). Thus the HDFs showed a rapid response to food resources in the warm eddies, and were influenced by biological processes.

4.3. Coupling between other physical processes and HDFs in the northern SCS

In the present study, HDF abundance and biomass were high in the estuarine system in both seasons, and HDF biomass correlated positively with Chl.*a* and nitrate but negatively with salinity in the mixing layer (Table 2). This might have indicated that the distribution of HDFs was influenced by the Pearl River as well as other coastal waters with high nutrients and Chl.*a* and low salinity. However, the vertical distribution of HDFs was quite different in the Pearl River estuary between the two seasons, which might be due to different mixing strength. In winter, there is lowest runoff in the Pearl River, and thus the water column of the estuary was occupied by seawater with high salinity (Huang et al., 2008). Homogeneity of HDF biomass in the water column at estuarine stations might be due to strong mixing water. In summer, there is the highest runoff in the Pearl River during the year, and the freshwater and seawater became stratified in both estuarine and coastal waters. The outflow of the Pearl River causes a very high phytoplankton biomass at Stn. A9, which is dominated by nano- and micro-phytoplankton (Huang et al., 2008). Large HDFs represented a high proportion of the total HDF biomass (Fig. 4), which may have resulted from a high proportion of nano- and micro-phytoplankton biomass. This suggested that the HDFs showed a rapid response to phytoplankton growth, and phytoplankton biomass might be an important factor influencing HDF abundance and distribution in the northern SCS.

Table 3
Pearson correlation coefficients between heterotrophic dinoflagellate (HDF) biomass and phytoplankton biomass (PB, Chl.*a*) in the northern South China Sea during cruises in February and July 2004. Significant correlation was defined as: [a]$p < 0.05$; [b]$p < 0.01$. Pico, <2 μm; nano, 2–20 μm; micro 20–200 μm. HDF, small, ≤20 μm; large, >20 μm.

HDF	Pico PB	Nano PB	Micro PB	Total PB	*n*
Feb. 2004					
Small	0.611[b]	0.539[b]	0.183	0.687[b]	78
Large	0.369[b]	0.685[b]	0.415[b]	0.492[b]	
Total	0.558[b]	0.710[b]	0.279[a]	0.653[b]	
Jul. 2004					
Small	0.561[b]	0.439[b]	0.235	0.497[b]	67
Large	0.296[a]	0.658[b]	0.585[b]	0.698[b]	
Total	0.538[b]	0.626[b]	0.495[b]	0.613[b]	

Table 4
Abundance and biomass of heterotrophic dinoflagellates (HDFs) and contribution of small HDFs (≤20 μm) in several tropical and temperate marine regions.

Study regions	Study time	Abundance (cells mL^{-1})	Biomass (μg C L^{-1})	Abundance[a] (%)	Biomass[a] (%)	References
Estuary and coast						
Coast of Chile	Oct–Dec 2004	59–104	–[b]	80[c]	–[b]	Masquelier and Vaulot, 2007
Gyeonggi Bay, Yellow Sea	1997–1999	4–95	0.6–71.2	89–94[c, d]	38.3[c]	Yang et al., 2008
Coast of Washington USA	Sep 2003	93–109	14.0–28.7	96–99	51[c]	Olson et al., 2006
Coast of northern SCS	Feb, July 2004	10–142	6.1–34.1	90–94	30–55	Present study
Continental shelf						
Mejillones Bay off Chile	Feb, Aug and Oct 2001	–[b]	0–1658[e]	–[b]	–[b]	Vargas and Gonzalez, 2004
Andaman Sea, Indian Ocean	Mar and Aug 1996	34–131[c]	–[b]	97–99[c]	–[b]	Nielsen et al., 2004
Offshore of Washington USA	Sep 2003	26–116	6.4–23.4	95–98	40–85	Olson et al., 2006
Shelf of northern SCS	Feb, July 2004	6–90	1.6–11.5	92–98	47–72	Present study
Open ocean						
Equatorial Pacific	Feb–Apr, Aug–Oct 1992	3–30	0.4–3.6	99	87–99	Verity et al., 1996
North Equatorial Pacific	Jul 1998	2.7–46	0.3–4.0	88–98	–[b]	Yang et al., 2004
Sargasso Sea	Aug 1989; Mar–Apr 1990	1–29	0.1–2.1	>92	18–78	Lessard and Murrell, 1996
Slope of northern SCS	Feb, July 2004	2–54	0.2–4.6	94–99	54–80	Present study

[a] Contribution of small HDFs.
[b] No data.
[c] Mean values.
[d] Use the value athecate HDF/total HDF, most of athecate were <20 μm.
[e] mg C m^{-2}.

Vertical distribution of HDFs on the continental shelf and slope showed that they were mostly concentrated near the bottom and sub-surface respectively, and this was associated with stratification in the water-column structure. Monsoons, and particularly their wind velocity, influenced water-column structure, the vertical mixing layer, nutricline depth and the nutrients available in the northern SCS, and thus affected plankton biomass in the upper water (Tseng et al., 2005; Huang et al., 2008). In the present study, HDFs were concentrated in a deeper layer on the continental shelf in summer, and showed a significantly positive correlation with nutrients in the mixing layer (Table 2). The wind speed of the northeast monsoon is much higher in winter than that of the southwest monsoon in summer in the northern SCS (Liu et al., 2002; Tseng et al., 2005). This, combined with convective overturn, deepens the mixing layer in winter, increases the nutrient available, and thus fuels phytoplankton and nanoflagellate growth in the upper water in winter (Huang et al., 2008). In summer, there were highly stratified water columns and vertical thermoclines, which prevented nutrient supply to the upper water and reduced the food resources, thus decreasing HDF biomass indirectly in the shelf and slope systems.

4.4. Factors controlling spatial and temporal variations of HDFs in subtropical waters

The spatial variation of HDFs was far more variable than the temporal variation between the two seasons in the northern SCS (Table 1). Such a result was probably because the study region contains complex ecosystems, including estuary, coast, continental shelf and slope. Both phytoplankton and nanoflagellates are major prey for HDFs (e.g. Sherr and Sherr, 1994; Jeong, 1999; Calbet et al., 2001). The HDF biomass showed a significant correlation with Chl.*a* in the northern SCS ($p < 0.01$, Table 3). During the same cruises, phytoplankton and nanoflagellate abundance were also variable among regions, mainly due to the availability of nutrients in the mixing layer in the northern SCS (Huang et al., 2008). The variations of HDF biomass among different ecosystems were probably caused by the availability of HDF prey, which in turn was mainly influenced by the nutrients available (Huang et al., 2008). The spatial distribution trends of the HDFs matched well those of Chl.*a* and nanoflagellates in the northern SCS (Huang et al., 2008), as well as the nutrients in the mixing layer. All of these results suggested that food resources seemed to be the major factor controlling the spatial distribution of HDFs in the study area.

The variation pattern of HDFs between winter and summer depended on the regions in the northern SCS. Thus, in estuarine and coastal regions, HDF biomass was higher in the summer ($p < 0.05$). In this region, phytoplankton biomass and nanoflagellates also had high values (Huang et al., 2008) as well as the nitrate in the mixing layer. On the continental slope, variation of the HDFs between the two seasons was unlike that in coastal water and on the continental shelf, with high biomass in winter but low in summer ($p < 0.01$). Temporal variation in the slope waters of the northern SCS agreed well with the variation of Chl.*a* and nanoflagellates (Tseng et al., 2005; Huang et al., 2008). Consequently, food resources, especially the phytoplankton biomass, seemed to be the major factor controlling spatial distribution and temporal variation of the HDFs in the northern SCS.

5. Conclusion

HDFs were ubiquitous in the northern SCS but decreased from the estuary to inshore and then offshore, with comparable abundance and biomass to other similar regions. Various physical processes (e.g. river outflow and monsoon), associated with biological processes in different systems, contributed to different seasonal variation and vertical profile patterns between the coast and slope regions. Warm eddies significantly affected the biomass and distribution of the HDFs in the northern SCS, but not in the same way due to their different characteristics. The distribution and seasonal variation of the HDFs accorded well with that of Chl.*a* and the nanoflagellates, and bottom-up (food resources) control had a significant influence on the HDFs in the northern SCS.

Acknowledgments

The authors would like to thank the captain and crew of R/V "Yanping 2" for their concerted efforts during field sampling, and Professor John Hodgkiss of The University of Hong Kong for polishing the English. This work was supported by China NSF (No. 40730846, 40806058, 90711006). This work was also supported by the National Basic Key Research Program of the Ministry of Science and Technology of China (China GLOBEC-IMERS Program, No. 2006CB400604).

References

Archer, S.D., Leakey, R.J.G., Burkill, P.H., Sleigh, M.A., 1996. Microbial dynamics in coastal waters of East Antarctica: herbivory by heterotrophic dinoflagellates. Marine Ecology Progress Series 139, 239–255.

Assmy, P., Henjes, J., Klaas, C., Smetacek, V., 2007. Mechanisms determining species dominance in a phytoplankton bloom induced by the iron fertilization experiment EisenEx in the Southern Ocean. Deep-Sea Research I 54, 340–362.

Benitez-Nelson, C.R., Bidigare, R.R., Dickey, T.D., Landry, M.R., Leonard, C.L., Brown, S.L., Nencioli, F., Rii, Y.M., Maiti, K., Becker, J.W., Bibby, T.S., Black, W., Cai, W., Carlson, C.A., Chen, F., Kuwahara, V.S., Mahaffey, C., McAndrew, P.M., Quay, P.D., Rappé, M.S., Selph, K.E., Simmons, M.P., Yang, E.J., 2007. Mesoscale eddies drive increased silica export in the subtropical Pacific Ocean. Science 316, 1017–1121.

Calbet, A., Landry, M.R., Nunnery, S., 2001. Bacteria–flagellate interactions in the microbial food web of the oligotrophic subtropical North Pacific. Aquatic Microbial Ecology 23, 283–292.

Chou, H.C., Gong, G.C., Kao, S.J., Chang, J., 2005. Cross-shelf distribution of summer dinoflagellate abundance in the east China Sea and its correlation to environmental factors. Journal of Fish Society of Taiwan 32, 87–100.

de Souza, R.B., Mata, M.M., Garcia, C.A.E., Kampel, M., Oliveira, E.N., Lorenzzetti, J.A., 2006. Multi-sensor satellite and in situ measurements of a warm core ocean eddy south of the Brazil–Malvinas Confluence region. Remote Sensing of Environment 100, 52–66.

Falkowski, P.G., Ziemann, D., Kolber, Z., Bienfang, P.K., 1991. Role of eddy pumping in enhancing primary production in the ocean. Nature 352, 55–58.

Froneman, P.W., Perissinotto, R., 1996. Structure and grazing of the micro-zooplankton communities of the subtropical convergence and a warm-core eddy in the Atlantic sector of the Southern Ocean. Marine Ecology Progress Series 135, 237–245.

Hall, J., Safi, K., Cumming, A., 2004. Role of micro-zooplankton grazers in the subtropical and subantarctic waters to the east of New Zealand. New Zealand Journal of Marine and Freshwater Research 38, 91–101.

Hlaili, A.S., Grami, B., Mabrouk, H.H., Gosselin, M., Hamel, D., 2006. Phytoplankton growth and micro-zooplankton grazing rates in a restricted Mediterranean lagoon (Bizerte Lagoon, Tunisia). Marine Biology 151, 767–783.

Henjes, J., Assmy, P., Klaas, C., Verity, P., Smetacek, V., 2007. Response of micro-zooplankton (protists and small copepods) to an iron-induced phytoplankton bloom in the Southern Ocean (EisenEx). Deep-Sea Research I 54, 363–384.

Huang, B.Q., Hong, H., Wang, H., 1999. Size-Fractionated primary productivity and the phytoplankton–bacteria relationship in the Taiwan Strait. Marine Ecology Progress Series 183, 29–38.

Huang, B.Q., Lan, W.L., Cao, Z.R., Dai, M.H., Huang, L.F., Jiao, N.Z., Hong, H.S., 2008. Spatial and temporal distribution of nanoflagellates in the northern South China Sea. Hydrobiologia 605, 143–157.

Huang, B.Q., Hu, J., Xu, H.Z., Dai M.H., Cao Z.R., Wang D.X. Phytoplankton community at warm eddies in the northern South China Sea in winter 2003/2004. Deep-Sea Research II, in press.

Jeong, H.J., 1999. The ecological roles of heterotrophic dinoflagellates in marine planktonic community. Journal of Eukaryotic Microbiology 46, 390–396.

Jia, Y.L., Liu, Q.Y., Liu, W., 2005. Primary studies of the mechanism of eddy shedding from the Kuroshio bend in Luzon Strait. Journal of Oceanography 61, 1017–1027.

Knap, A., Michaels, A., Close, A., Ducklow, H., Dickson, A. (Eds.), 1996. Protocols for the Joint Global Ocean Flux Study (JGOFS) Core Measurements. JGOFS Report Nor. 19, Reprint of the IOC Manuals and Guides No. 29, UNESCO 1994, vi + 170 pp.

Lessard, E.J., 1991. The trophic role of heterotrophic dinoflagellates in diverse marine environments. Marine Microbial Food Webs 5, 49–58.

Lessard, E.J., Murrell, M.C., 1996. Distribution, abundance and size composition of heterotrophic dinoflagellates and ciliates in the Sargasso Sea near Bermuda. Deep-Sea Research I 43, 1045–1065.

Levinsen, H., Nielsen, T.G., 2002. The trophic role of marine pelagic ciliates and heterotrophic dinoflagellates in arctic and temperate coastal ecosystems. A cross-latitude comparison. Limnology and Oceanography 47, 427–439.

Lewis, M.R., 2002. Variability of plankton and plankton processes on the mesoscale. In: Williams, PJLe.B., Thomas, D.N., Reynolds, C.S. (Eds.), Phytoplankton Productivity—Carbon Assimilation in Marine and Freshwater Ecosystems. Blackwell Science, Malden, Mass, pp. 141–155.

Liu, K.K., Chao, S.Y., Shaw, P.T., Gong, G.C., Chen, C.C., Tang, T.Y., 2002. Monsoon-forced chlorophyll distribution and primary production in the South China Sea: observations and a numerical study. Deep-Sea Research I 49, 1387–1412.

Mackas, D.M., Galbraith, M., 2002. Zooplankton distribution and dynamics in a North Pacific eddy of coastal origin: I. contributions. Transport and loss of continental species. Journal of Oceanography 58, 725–738.

Masquelier, S., Vaulot, D., 2007. Distribution of micro-organisms along a transect in the South-East Pacific Ocean (BIOSOPE cruise) from epifluorescence microscopy. Biogeosciences Discussion 4, 2667–2697.

McGillicuddy, D.J., Anderson, L.A., Bates, N.R., Bibby, T., Buesseler, K.O., Carlson, C.A., Davis, C.S., Ewart, C., Falkowski, P.G., Goldthwait, S.A., Hansell, D.A., Jenkins, W.J., Johnson, R., Kosnyrev, V.K., Ledwell, J.R., Li, Q.P., Siegel, D.A., Steinberg, D.K., 2007. Eddy/wind interactions stimulate extraordinary mid-ocean plankton blooms. Science 316, 1021–1126.

McGillicuddy, D.J., Robinson, A.R., 1997. Eddy-induced nutrient supply and new production in the Sargasso Sea. Deep-Sea Research I 44, 1427–1450.

Menden-Deuer, S., Lessard, E.J., 2000. Carbon to volume relationships for dinoflagellates, diatoms and other protist plankton. Limnology and Oceanography 45, 569–579.

Nielsen, T.G., Andersen, C.M., 2002. Plankton community structure and production along a freshwater-influenced Norwegian fjord system. Marine Biology 141, 707–724.

Nielsen, T.G., Bjornsen, P.K., Boonruang, P., Fryd, M., Hansen, P.J., Janekarn, V., Limtrakulvong, V., Munk, P., Hansen, O.S., Satapoomin, S., Sawangarreruks, S., Thomsen, H.A., Ostergaard, J.B., 2004. Hydrography, bacteria and protist communities across the continental shelf and shelf slope of the Andaman Sea (NE Indian Ocean). Marine Ecology Progress Series 274, 69–86.

Ning, X., Chai, F., Xue, H., Cai, Y., Liu, C., Shi, J., 2004. Physical–biological oceanographic coupling influencing phytoplankton and primary production in the South China Sea. Journal of Geophysical Research 109, C10005. doi:10.1029/2004JC002365.

Olson, M.B., Lessard, E.J., Wong, C.H.J., Berhhardt, M.J., 2006. Copepod feeding selectivity strongly influences the population ecology of the microplankton, including the toxigenic diatom, *Pseudo-nitzschia* spp., in the coastal Pacific Northwest. Marine Ecology Progress Series 326, 207–220.

Pai, S.C., Yang, C.C., Riley, J.P., 1991. Effects of acidity and molybdate concentration on the kinetics of the formation of the phosphoantimonylmolybdenum blue complex. Analytica Chimica Acta 229, 115–120.

Parsons, T.R., Yoshiaki, M., Lalli, C.M., 1984. A Manual of Chemical and Biological Methods for Seawater Analysis. Pergamon Press, Oxford.

Paterson, H.L., Knott, B., Waite, A.M., 2007. Micro-zooplankton community structure and grazing on phytoplankton, in an eddy pair in the Indian Ocean off Western Australia. Deep-Sea Research II 54, 1076–1093.

Rat'kova, T.N., Wassmann, P., 2002. Seasonal variation and spatial distribution of phyto- and protozooplankton in the central Barents Sea. Journal of Marine Systems 38, 47–75.

Rodríguez, F., Varela, M., Fernández, E., Zapata, M., 2003. Phytoplankton and pigment distributions in an anticyclonic slope water oceanic eddy (SWODDY) in the southern Bay of Biscay. Marine Biology 143, 995–1011.

Sherr, E.B., Sherr, B.F., 1994. Bacterivory and herbivory: key roles of phagotrophic protists in pelagic food webs. Microbial Ecology 28, 223–235.

Sherr, E.B., Sherr, B.F., Fessenden, L., 1997. Heterotrophic protists in the central Arctic ocean. Deep-Sea Research II 44, 1665–1682.

Sherr, E.B., Sherr, B.F., 2007. Heterotrophic dinoflagellates: a significant component of micro-zooplankton biomass and major grazers of diatoms in the sea. Marine Ecology Progress Series 352, 187–197.

Stelfox, C.E., Burkill, P.H., Edwards, E.S., Harris, R.P., Sleigh, M.A., 1999. The structure of zooplankton communities, in the 2 to 2000 μm size range, in the Arabian Sea during and after the SW monsoon, 1994. Deep-Sea Research II 46, 815–842.

Tseng, C.M., Wong, G.T.F., Lin, I.I., Wu, C.R., Liu, K.K., 2005. A unique seasonal pattern in phytoplankton biomass in low-latitude waters in the South China Sea. Geophysical Research Letters 32, L08608. doi:10.1029/2004GL022111.

Vargas, C.A., Gonzalez, H.E., 2004. Plankton community structure and carbon cycling in a coastal upwelling system. II. Microheterotrophic pathway. Aquatic Microbial Ecology 34, 165–180.

Verity, P.G., Stoecker, D.K., Sieracki, M.E., Nelson, J.R., 1996. Micro-zooplankton grazing of primary production at 140°W in the equatorial Pacific. Deep-Sea Research II 43, 1227–1255.

Wang, D., Xu, H., Lin, J., Hu, J., 2008. Anticyclonic eddies in the northeastern South China Sea during winter 2003/2004. Journal of Oceanography 64, 925–935.

Wang, G.H., Su, J.L., Chu, P.C., 2003. Mesoscale eddies in the South China Sea observed with altimetry. Geophysical Research Letters 30, 2121. doi:10.1029/2003GL018532.

Yang, E.J., Choi, J.K., Hyun, J.H., 2004. Distribution and structure of heterotrophic protist communities in the northeast equatorial Pacific Ocean. Marine Biology 146, 1–15.

Yang, E.J., Choi, J.K., Hyun, J.H., 2008. Seasonal variation in the community and size structure of nano- and micro-zooplankton in Gyeonggi Bay, Yellow Sea. Estuarine, Coastal and Shelf Science 77, 320–330.